

# PHASE DETERMINATION OF X-RAY REFLECTIONS FOR MEMBRANE-TYPE SYSTEMS WITH CONSTANT FLUID DENSITY

J. B. STAMATOFF *and* S. KRIMM

*From the Department of Physics, and Biophysics Research Division,  
Institute of Science and Technology, University of Michigan,  
Ann Arbor, Michigan 48104. Dr. Stamatoff's present address is  
Bell Laboratories, Murray Hill, New Jersey 07974.*

**ABSTRACT** A new technique for phase determination of X-ray reflections from symmetric structures is presented. This method, involving comparison of intensity data from structures with variable fluid layer thickness and constant fluid electron density, permits computation of phase angles, scaling factors, and origin reflection values independently. Possible sources of error inherent in other methods of phase determination are thereby eliminated. Results of the application of this method to model structures and to myelin data are reported. Advantages of the technique, which tests all possible phase angle combinations in a rapid fashion, are discussed.

## INTRODUCTION

Structural information obtained from biological membranes or lipid bilayers by X-ray diffraction analysis is based predominantly on the ability to compute projected electron density distributions. This computation requires a solution of the phase problem, which is often simplified by the assumption that the phase angles are restricted to 0 or  $\pi$  radians. This constraint is equivalent to assuming that the projected electron density distribution is symmetric, which is reasonable for stacks of membrane pairs which are created by the collapse of intact vesicles, or for lipid multilayers.

Solution of this restricted phase problem or its equivalent has been attempted by a variety of techniques, including applications of the sampling theorem (Worthington et al., 1973), direct deconvolution methods (Worthington et al., 1973; Pape, 1974), or a combination of both approaches (Moody, 1974). Direct deconvolution methods require a set of intensities of reflections for only one periodicity,  $D$ . However, the requirement of this method that  $D \geq 2W$ , where  $W$  is the width of a symmetric pair of membranes, limits the diffraction experiments to samples containing thick intermembrane pair fluid layers. For stacks of membranes created from isolated membrane vesicles, these thick layers of fluid often permit considerable stacking disorder, which lowers the resolution obtainable in the pattern. Other deconvolution methods require that the number of unit cells be small (Hosemann and Bagchi, 1962). This causes broadening of the diffraction maxima, which also usually limits the experimentally ob-

tainable resolution. A general Patterson analysis of samples containing some disorder has permitted the membrane pair autocorrelation function to be obtained in some cases, to which direct deconvolution methods have been applied (Schwartz et al., 1974). The sampling theorem approach (Worthington et al., 1973) and the novel application of both the sampling theorem approach and direct deconvolution methods (Moody, 1974) require at least two sets of intensities, from two different periodicities. Therefore, scaling factors between these sets of intensities must be known.

The theory presented below shows that phase angles can be determined without a priori knowledge of these scaling factors or of the unobserved origin reflection. The technique is an extension of the concepts of the Worthington et al. (1973) method of real space comparison of electron densities, the Luzzati et al. (1972) image recognition procedure, and the approach used by Corless (1972).

### THEORY

Let  $\rho_m(x, y, z)$  be the electron density distribution of a single membrane on a scale where the surrounding fluid electron density is set equal to zero. The projected electron density distribution is defined as

$$\rho_m(z) = \iint_{-\infty}^{+\infty} \rho_m(x, y, z) dx dy,$$

where the  $z$  axis is orthogonal to the plane of the membrane.  $\rho_m(z)$  is, in general, an asymmetric function that is non-zero over a finite range in  $z$ . The projected electron density distribution of the double membrane pair produced by the collapse of an intact vesicle is,

$$\rho(z) = \rho_m(z) * \delta[z - (D_S/2)] + \rho_m(-z) * \delta[z + (D_S/2)],$$

where  $*$  indicates convolution,  $\delta$  is a Dirac delta function, and  $D_S$  is the separation of membranes within the pair. Thus,  $\rho(z)$  must be a symmetric function.

Define

$$F(S) \leftrightarrow \rho(z),$$

where  $\leftrightarrow$  indicates a Fourier transform pair. Let the double membrane pair be placed in a one dimensional lattice of periodicity  $D$ . Then the electron density distribution of this lattice is given by

$$\rho_P(z) = \rho(z) * \sum_{n=-\infty}^{+\infty} \delta(z - nD),$$

and

$$\sum_{h=-\infty}^{+\infty} F(h/D) \delta(S - h/D) \leftrightarrow \rho_P(z)$$

Thus the values of  $\{F(h/D)\}$  sample the real function  $F(S)$ , and the set of intensities  $\{I(h/D)\}$  (where  $I(h/D) = F^2(h/D)$ ) are the observables for the periodicity  $D$ . We will assume that  $\rho(z)$  (and therefore  $\rho_m(z)$ ,  $D_S$ , and  $F(S)$ ) remains unchanged on swelling. The constant  $\rho(z)$  may refer to a membrane pair for which either the cytoplasmic or intracellular sides of the membranes oppose one another. The following theory also applies to the special case in which  $\rho_m(z)$  is symmetric and  $D_S = D/2$ . This case holds for the erythrocyte membrane (Stamatoff et al., 1975) in which the recorded periodicity is too small to correspond to the periodic arrangement of double membrane pairs (for which  $\rho_m(z)$  is symmetric and  $D_S \neq D/2$  or  $\rho_m(z)$  is asymmetric for any  $D_S$  consistent with  $D$ ).

If two infinite sets of intensities  $\{I(h/D_1)\}$  and  $\{I(h/D_2)\}$  could be obtained, then the signs of  $F(h/D)$  could be derived by previous methods. However, the experimentally obtainable intensities are  $\{I(h/D_1)\}$  and  $\{I_o(h/D_2)\}$ , where  $h_{\max}$  is finite,  $h \neq 0$ , and  $I(h/D_2) = A^2 I_o(h/D_2)$ . Thus the origin reflection,  $I(0)$ , and scaling constant,  $A$ , remain unknown. In addition, the intensity data are truncated.

In order to circumvent this problem, consider the electron density functions derived without using the origin reflection

$$\rho_{P1}(z) = (2/D_1) \sum_{h=1}^{\infty} (\pm) \sqrt{I(h/D_1)} \cos[2\pi(h/D_1)z] \quad (1)$$

and

$$\rho_{P2}(z) = (2/D_2) \sum_{h=1}^{\infty} (\pm) \sqrt{I_o(h/D_2)} \cos[2\pi(h/D_2)z]. \quad (2)$$

Both functions will change for each combination of signs of the reflections. For the correct combination of signs, however, the same  $\rho(z)$  must be obtained from both sets of reflections. This is given by

$$\rho(z) = \rho_{P1}(z) + [F(0)/D_1] = A\rho_{P2}(z) + [F(0)/D_2]$$

for  $|z| \leq D_1/2 < D_2/2$ . So that,

$$\rho_{P1}(z) = A\rho_{P2}(z) + B, \quad (3)$$

where  $B = F(0)[(D_1 - D_2)/(D_1 D_2)]$  for  $|z| \leq D_1/2 < D_2/2$ . Thus a plot of  $\rho_{P2}(z)$  vs.  $\rho_{P1}(z)$  will produce a straight line, for the correct combination of signs, whose slope is the scaling factor and whose intercept is a function of  $F(0)$ .

Eq. 3 may be used to obtain the correct combination of signs. Each combination may be compared by computing the mean square deviation from a straight line. The deviation is

$$\Delta = \sum_{i=1}^N [\rho_{P1}(z_i) - A\rho_{P2}(z_i) - B]^2 / \sum_{i=1}^N [\rho_{P1}(z_i)]^2 \quad (4)$$

for  $|z_i| \leq D_1/2 < D_2/2$ .  $A$  and  $B$  are determined by the conditions,

$$\partial \Delta / \partial A = 0 \quad \text{and} \quad \partial \Delta / \partial B = 0$$

to be,

$$A = \left[ N \sum_{i=1}^N \rho_{P1}(z_i) \rho_{P2}(z_i) - \sum_{i=1}^N \rho_{P1}(z_i) \sum_{i=1}^N \rho_{P2}(z_i) \right] / \left[ N \sum_{i=1}^N [\rho_{P2}(z_i) - \bar{\rho}_{P2}]^2 \right],$$

and  $B = \bar{\rho}_{P1} - A \bar{\rho}_{P2}$ , where

$$\bar{\rho}_{P1} = (1/N) \sum_{i=1}^N \rho_{P1}(z_i)$$

and

$$\bar{\rho}_{P2} = (1/N) \sum_{i=1}^N \rho_{P2}(z_i).$$

This computation has been successfully tested with models and applied to experimental data obtained from human erythrocyte membranes (Stamatoff, 1974). The calculation involves computation of  $N$  electron density points for each set of data using Eqs. 1 and 2 for all possible combinations of signs. This calculation, however, may become lengthy and compares only  $N$  electron density points.

A deviation based upon a comparison of all points in the unit cell may be defined as

$$\Delta = \int_{-D_1/2}^{+D_1/2} [\rho_{P1}(z) - A \rho_{P2}(z) - B]^2 dz / \int_{-D_1/2}^{+D_1/2} [\rho_{P1}(z)]^2 dz, \quad (5)$$

which is a generalization of Eq. 4. Substituting Eqs. 1 and 2 into Eq. 5 and noting that,

$$\int_{-D_1/2}^{+D_1/2} (A \rho_{P2}(z) + [F(0)/D_2])^2 dz = \int_{-D_2/2}^{+D_2/2} (A \rho_{P2}(z) + [F(0)/D_2])^2 dz,$$

(i.e. the fluid density is zero for  $D_1/2 < |z| \leq D_2/2$ ) results in the following expressions:

$$\Delta = (\gamma_0 + A^2 \gamma_1 - A \gamma_2 - B^2 [D_2 D_1 / (D_1 - D_2)] - AB \gamma_3) \gamma_0^{-1} \quad (6)$$

and

$$A = \gamma_2 (2\gamma_1 + [\gamma_3^2/2] [(D_1 - D_2)/D_1 D_2])^{-1},$$

$$B = \frac{1}{2} \gamma_3 A [(D_2 - D_1)/D_2 D_1],$$

where

$$\gamma_0 = 2 \sum_{h=1}^{\infty} [F^2(h/D_1)/D_1],$$

$$\gamma_1 = 2 \sum_{h=1}^{\infty} [F_0^2(h/D_2)/D_2]$$

$$\gamma_2 = 4 \sum_{h,k=1}^{\infty} \frac{F(h/D_1)F_0(k/D_2)}{D_2} \left( j_0 \left[ \pi D_1 \left( \frac{h}{D_1} - \frac{k}{D_2} \right) \right] + j_0 \left[ \pi D_1 \left( \frac{h}{D_1} + \frac{k}{D_2} \right) \right] \right),$$

$$\gamma_3 = 4 \sum_{k=1}^{\infty} [F_0(k/D_2)D_1/(D_1 - D_2)] j_0[\pi(D_1/D_2)k],$$

and  $j_0(x) = \sin(x)/x$ ,  $F_0^2(k/D_2) = I_0(k/D_2)$ ,  $F^2(h/D_1) = I(h/D_1)$ . Although these expressions are more formidable than the previous sums, the calculation of  $\Delta$  is much more rapid by computer and has the advantage that all electron density points are considered.

In practice,  $\Delta$  is computed for each combination of signs. The computer then sorts the combinations, slopes, and intercepts, according to increasing  $\Delta$ . For two sets of six reflections there are  $2^{12}$  combinations. Because  $\rho(z)$  and  $-\rho(z)$  cannot be distinguished in this or other swelling theories, there are  $2^{11}$  or 2,048 combinations to be tested. On the IBM 370/168 this takes 0.64 s of CPU time.

A two set comparison (although not displayed) may be envisaged as a two-dimensional plot. The deviations  $\Delta_{ij}$  may be considered to be elements of a two-dimensional array in which  $i$  refers to a sign combination for one set of data,  $j$  refers to the sign combination for the other set, and slopes ( $A_{ij}$ ) and intercepts ( $B_{ij}$ ) are associated with each  $\Delta_{ij}$ . For a three (or more) set comparison, a three (or more) dimensional plot and array may be envisaged. However, calculations corresponding to this method take too long. For example, for three sets of six reflections each there are  $2^5 \cdot 2^6 \cdot 2^6 = 2^{17}$  distinguishable combinations. We therefore proceed as follows. For this situation, one set is chosen as the basis set. For each sign combination of the basis set, the smallest deviations for all possible sign combinations of each of the other sets is calculated. These deviations are then averaged and the averaged or global deviation,  $\Delta_G$ , is sorted by the computer according to increasing  $\Delta_G$ . Thus all possible sign combinations of all sets are tested including all possible combinations for the basis set.

## MODEL CALCULATIONS

Model calculations were performed as a test of the above method of determining phases. The following models were considered.

*Model I: Step Function.*  $\rho(z) = 1$  if  $|z| \leq 25 \text{ \AA}$ ;  $\rho(z) = 0$  otherwise.

*Model II: Luzzati Function.*  $\rho(z) = \frac{1}{2}(A \exp(-e(z-a)^2) + A \exp(-e(z+a)^2) - B \exp(-gz^2))$ , where  $A = 0.145$ ,  $B = -0.091$ ,  $a = 35.6 \text{ \AA}$ ,  $e = 0.120 \text{ \AA}^{-2}$ , and  $g = 0.0156 \text{ \AA}^{-2}$ .

*Model III: Peak Function.*  $\rho(z) = \cos(2\pi z/x)$  for  $|z| \leq 25 \text{ \AA}$  and  $\rho(z) = 0$  otherwise, where  $x = 19 \text{ \AA}$ .

For each model,  $\rho(z)$  may be considered to be either the electron density distribution

for a double membrane pair or for a single symmetric membrane for which  $D_S = D/2$  as mentioned previously. Model I is very dissimilar to current concepts of membrane projected electron density distributions. Model II was reported by Rand and Luzzati (1968) as the result of an X-ray diffraction study on lipids extracted from human erythrocyte membranes. It might be expected to be similar to a single membrane projected electron density distribution. Model III has a Fourier transform with a dominant peak at  $1/19 \text{ \AA}^{-1}$ .

The results of our method when applied to two sets of "data" from model I are shown in Table I. The inputs to the computer are the magnitudes of the reflections  $|F(h/D)|$  for two different periodicities (i.e., scaling changes were not made). All sign combinations are tested, and it is found that the smallest deviation corresponds to the correct sign combinations. The first occurrence of a situation in which the two sets differ in sign combination is found in the 13th position. The results for this combination are also given in Table I.

Table II shows the results of a four set comparison for model I, again not altering the scaling. The sign combinations corresponding to the smallest global deviation are the correct ones. The second and third comparisons which are shown required (by the method of averaging) that the basis set change sign combination. However, all combinations are tested. This means that the first comparison has the smallest value of  $\Delta_G$  but other combinations may have  $\Delta_G$  values between the first and second comparisons.

Table III is a summary of similar calculations performed on all three models. The sign combinations shown in the third column ranked first in each calculation, and are seen to be the correct ones. Origin reflection values were calculated using Eq. 3. Scaling factors are in good agreement with actual ones, but origin reflection values show large variations. Global deviations are given in the last column. Perfect con-

TABLE I  
CALCULATION OF PHASES FOR THE STEP FUNCTION: TWO PERIODICITIES

Periodicity	Deviation $\times 10^2$	Slope	Intercept $\times 10^2$	Signs of reflections*
<i>A</i>				
55.0	Basis set	—	—	+ - + - + -
58.0	2.226	1.096	-5.907	+ - + - + -
55.0	Basis set	—	—	+ - + - + -
58.0	6.431	0.923	-4.023	+ - + - + -
55.0	Basis set	—	—	+ - + - + -
58.0	7.308	0.867	-3.290	+ - + - + -
55.0	Basis set	—	—	+ - + - + -
58.0	7.669	0.784	-1.738	+ - + - + -
13th position				
55.0	Basis set	—	—	+ - + - + -
58.0	10.16	0.966	-4.717	+ - + - + -

\*Ranked according to increasing  $\Delta$ .

TABLE II  
CALCULATION OF PHASES FOR THE STEP FUNCTION: FOUR PERIODICITIES

Periodicity	Deviation $\times 10^2$	Slope	Intercept $\times 10^2$	Signs of reflections*
<i>A</i>				
55.0	3.981	1.015	4.374	+ - + - + -
58.0	Basis set	—	—	+ - + - + -
60.0	0.834	1.068	-3.664	+ - + - + -
65.0	0.826	1.004	-9.413	+ - + - + -
	$\Delta_G = 1.880$			
55.0	6.920	0.9996	4.307	+ - + - + -
58.0	Basis set	—	—	+ - + - + -
60.0	3.199	1.055	-3.620	+ - + - + -
65.0	2.889	1.050	-10.480	+ - + - + -
	$\Delta_G = 4.336$			
55.0	6.156	1.095	3.460	+ - + - + -
58.0	Basis set	—	—	+ - + - + -
60.0	3.597	1.010	-3.040	+ - + - + -
65.0	5.561	1.087	-11.340	+ - + - + -
	$\Delta_G = 5.105$			

\*Ranked according to increasing  $\Delta_G$ .

TABLE III  
PHASE CALCULATIONS FOR MODEL STRUCTURES

Periodicity	Signs of reflections		Scaling factor		Origin reflection		$\Delta_G$ ,* deviation $\times 10^2$
	Actual	Calculated	Actual	Calculated	Actual	Calculated	
<i>A</i>							
Luzzati function							
55.0	- - + - - +	- - + - - +	1.0	0.987	+0.0962	-0.0855	
58.0	- - + - - +	- - + - - +	1.0	Basis set	—	—	
60.0	- - + - - +	- - + - - +	1.0	1.005	+0.0962	-0.3280	0.639
65.0	- - + - - +	- - + - - +	1.0	0.994	+0.0962	+0.1428	(0.993)
Step function							
55.0	+ - + - + -	+ - + - + -	1.0	1.015	+50.0000	+46.5102	
58.0	+ - + - + -	+ - + - + -	1.0	Basis set	—	—	
60.0	+ - + - + -	+ - + - + -	1.0	1.068	+50.0000	+63.7536	1.880
65.0	+ - + - + -	+ - + - + -	1.0	1.004	+50.0000	+50.6957	(4.336)
Peak function							
55.0	- + + - - +	- + + - - +	1.0	0.998	+5.5385	+11.5265	
58.0	- + + - - +	- + + - - +	1.0	Basis set	—	—	
60.0	- + + - - +	- + + - - +	1.0	0.999	+5.5385	+2.0671	0.118
65.0	- + + - - +	- + + - - +	1.0	1.000	+5.5385	+4.6166	(0.762)

\*Values of global deviations for the second best set of signs for each comparison are given in parentheses.

TABLE IV  
PHASE CALCULATIONS FOR MODEL STRUCTURES: 10% ERRORS IN INTENSITY  
AND SCALE FACTOR CHANGES

Periodicity	Signs of reflections		Scaling factor		Origin reflection		$\Delta_G$ ,* deviation $\times 10^2$
	Actual	Calculated	Actual	Calculated	Actual	Calculated	
<i>A</i>							
Luzzati function							
55.0	---+--+	---+--+	1.333	1.280	+0.0962	-0.1247	
58.0	---+--+	---+--+	1.000	Basis set	—	—	1.032
60.0	---+--+	---+--+	4.000	3.896	+0.0962	-0.4032	(1.401)
65.0	---+--+	---+--+	0.500	0.517	+0.0962	+0.1231	
Step function							
55.0	+---+--	+---+--	4.000	3.836	+50.0000	44.7025	
58.0	+---+--	+---+--	1.000	Basis set	—	—	
60.0	+---+--	+---+--	2.000	2.018	+50.0000	60.7782	2.239
65.0	+---+--	+---+--	1.333	1.303	+50.0000	48.5037	(4.580)
Peak function							
55.0	+++++	+++++	0.286	0.268	+5.5385	+13.9084	
58.0	+++++	+++++	1.000	Basis set	—	—	
60.0	+++++	+++++	1.250	1.328	+5.5385	-0.2507	0.250
65.0	+++++	+++++	0.667	0.668	+5.5385	+5.6281	(1.013)

\*Values of global deviation for the second best set of signs for each comparison are given in parentheses.

sistency of the electron density would result in a zero value for the deviation. In order to judge the degree of consistency, the global deviation for the next best set of signs is given in parentheses for each calculation.

Table IV is a summary of calculations performed on the same three models, but with randomly introduced intensity errors and scale factor changes between sets of reflections. The errors were as large as 10% in intensity (5% of  $|F(h/D)|$ ). Scale factor changes between sets of reflections were arbitrarily chosen. Again sign combinations corresponding to the smallest global deviation for each calculation are the correct ones. The computed scale factors are in good agreement with actual ones, but the origin reflection values show large variations. Global deviations are reported in the same manner as described above.

The effects of progressive truncation of reflections are shown in Table V for two of the models. These, and calculations using model III with variable values for  $x$ , show that the correct sign combination results unless major variations in  $F(S)$  are not sampled.

A scaling formula derived by Blaurock (1967) has been used extensively in the derivation of phases. In this formula,

$$(1/D_1) \sum_{h=-\infty}^{+\infty} I(h/D_1) = (A^2/D_2) \sum_{h=-\infty}^{+\infty} I_o(h/D_2), \quad (7)$$

where the scaled reflections are  $F(h/D_2) = \pm A [I_o(h/D_2)]^{1/2}$ . This formula is strictly



TABLE V  
EFFECT OF TRUNCATION ON THE CALCULATED PHASES OF MODEL STRUCTURES

Periodicity	Signs of reflections		Scaling factor		Origin reflection		Deviation* ×10 <sup>2</sup>
	Actual	Calculated	Actual	Calculated	Actual	Calculated	
<i>A</i>							
Step function							
55.0	+ - + - + -	+ - + - + -	1.0	1.015	+50.0000	+46.5102	3.981
58.0	+ - + - + -	+ - + - + -	1.0	Basis set	—	—	(6.155)
55.0	+ - + - + -	+ - + - + -	1.0	1.077	+50.0000	+44.1496	3.814
58.0	+ - + - + -	+ - + - + -	1.0	Basis set	—	—	(4.050)
55.0	+ - + -	+ - - -	1.0	1.300	+50.0000	23.4146	2.672
58.0	+ - + -	+ - - -	1.0	Basis set	—	—	(3.161)
Luzzati function							
55.0	- - + - - +	- - + - - +	1.0	Basis set	—	—	0.943
58.0	- - + - - +	- - + - - +	1.0	1.003	+0.0962	-0.2655	(1.181)
55.0	- - + - -	- - + - -	1.0	Basis set	—	—	0.217
58.0	- - + - -	- - + - -	1.0	0.993	+0.0962	+0.0178	(0.457)
55.0	- - + -	- - + -	1.0	Basis set	—	—	1.132
58.0	- - + -	- - + -	1.0	1.021	+0.0962	+0.8936	(1.663)

\*Values of deviations for the second best set of signs for each comparison are given in parentheses.

correct. However, the actual experimental data are truncated, and the origin reflection is not observed. As a result, the formula which is actually used is

$$(1/D_1) \sum_{h=1}^{N_1} I(h/D_1) = (A'^2/D_2) \sum_{h=1}^{N_2} I_o(h/D_2). \quad (8)$$

The results shown in Table VI are from a calculation comparable to those previously

TABLE VI  
PHASE CALCULATION FOR THE STEP FUNCTION USING THE  
BLAUROCK SCALING FORMULA

Periodicity	Deviation ×10 <sup>2</sup>	Slope	Intercept ×10 <sup>2</sup>	Signs of reflection*
<i>A</i>				
55.0	Basis set	—	—	+ - - - -
58.0	7.671	0.7802	-1.730	+ - - - -
55.0	Basis set	—	—	+ - + + +
58.0	8.245	0.7802	-2.959	+ - + + +
55.0	Basis set	—	—	+ - + + +
58.0	8.259	0.7802	-2.564	+ - + + +
55.0	Basis set	—	—	+ + + + +
58.0	8.408	0.7802	-0.535	+ + + + +
11th position				
55.0	Basis set	—	—	+ - - + -
58.0	10.35	0.7802	-4.204	+ - - + -

\*Ranked according to increasing Δ.

described, but in which the Blaurock scaling factor  $A'$  is used for the step function model and fixed during the calculation (i.e.  $A$  is not allowed to vary in the calculation of  $\Delta$  or  $B$  in Eq. 6). An incorrect combination of signs ranks first. It is not until the 11th position that the correct combination of signs is found.

## DISCUSSION

The model calculations show that the method developed in this paper clearly works. Sign combinations and scaling factors are correctly predicted. However, variation in the origin reflection value is considerable. Examination of Eq. 3 shows why this is the case: small changes in  $B$  will usually result in large changes in  $F(0)$ , due to the typically large values of  $[D_1 D_2 / (D_1 - D_2)]$ . Therefore  $F(0)$  is extremely sensitive to experimental or truncation errors. This is true even if  $F(0)$  is calculated via the sampling theorem in reciprocal space. Techniques which use consistency of  $F(0)$  calculated values as an indication of the correct choice of signs are therefore prone to error.

The calculations summarized in Table VI show the possibility that sign combination errors may result by omitting  $I(0)$  in the Blaurock formula. Comparing Eqs. 7 and 8 and taking  $N_1$  and  $N_2$  to be the truncation points in Eq. 7 also, the following relation holds,

$$A^2/A'^2 = 1 - \frac{1}{2}I(0)[(D_1 - D_2)/D_2] \left( \sum_{h=1}^{N_1} I(h/D_1) \right)^{-1}, \quad (9)$$

where  $I(0)$  is the actual origin reflection and  $I(0) = A^2 I_o(0)$ . Thus, if  $I(0)$  is large compared with other observed reflections, an appreciable scaling factor change may occur. This change can then result in sign combination errors by any method of analysis and particularly for weak reflections. The relative magnitude of  $I(0)$  is therefore important and not the absolute magnitude. The relative magnitude depends upon the shape of the electron density distribution. Therefore arguments which justify the neglect of  $I(0)$  based upon the necessarily small absolute magnitudes of  $I(0)$  for biological membranes do not apply. An implication of such a calculation is that "membrane-type" profile electron density distributions may be the result of use of this scaling formula.

Inclusion of other sets of data reduces the magnitude of this problem. If four sets of step function data are scaled by the Blaurock formula in Eq. 8, and the scaling factors are fixed during the calculation, then the correct combination of signs results. However, this may not be the case for other models, particularly those with weak reflections. It should be noted that phase changes of weak reflections can alter the interpretation of an electron density distribution significantly.

Although there are cases where use of the Blaurock formula does not lead to error, there are also cases which result in error. Unless further information is known about the structure (e.g. the relative magnitude of  $I(0)$ ) the application of this formula remains uncertain.

TABLE VII  
CALCULATION OF PHASES FOR MYELIN DATA  
(From Blaurock, A.E. 1967. Ph.D. Thesis, University of Michigan)

Periodicity	Deviation $10^2$	Slope	Intercept $10^4$	Signs of reflections
<i>A</i>				
166.0*	7.942	0.9713	-0.412	++++
171.0†	Basis set	—	—	++++(-§)
252.0‖	3.384	0.9883	-9.494	+0++(-§)---
343.0§‖	8.271	0.9553	-2.415	0-++++(-§)---
	$\Delta_G = 6.532$			
166.0*	Basis set	—	—	++++
252.0‖	0.871	0.9676	0.818	(-§)0++++
343.0§‖	3.632	0.9667	-2.377	0-++++(-§)---
	$\Delta_G = 2.252$			
166.0*	Basis set	—	—	++++
171.0†	0.331	0.9862	0.429	++++

\*Myelin in 1 mM CaCl<sub>2</sub>.

†Myelin in Ringer's solution.

§Different than Blaurock, A.E. 1971. *J. Mol. Biol.* 56:35.

‖Myelin in water (the reported values were 252 Å and 342 Å. However 343 Å was used to avoid a "0 divide" problem in the computer program. This value should be well within experimental error.)

#### NERVE MYELIN CALCULATIONS

We have performed extensive calculations using data collected by Blaurock (1967) from frog sciatic nerve, and these are summarized in Table VII. The results shown correspond to three separate calculations on different groups of reflections, and show sign combinations for the minimum global deviations.

Differences between the magnitudes of the global deviations indicate that the starting assumption is invalid when applied to all four sets of data and that the structure has changed on swelling. In other words, the 166, 252, and 343 Å sets appear to sample one transform whereas the 166 and 171 Å sets lie on a different transform (the 166 Å set is on both transforms). This conclusion has been reported previously (Blaurock, 1971; King, 1971), and indicates differences in the crystallographic origin (i.e. swelling site) of myelin under the various experimental conditions used. The sign combinations for the last two comparisons are almost equivalent to those reported by Blaurock (1971) and Worthington and King (1971) (noting the change in origin). Therefore the use of the Blaurock scaling formula did not produce a major difference in this case. In summary, application of this method to myelin data support the choice of signs made by Blaurock (1971) and Worthington and King (1971) provided the assumption of constant  $\rho(z)$  is applicable for the last two comparisons shown in Table VII.

Figs. 1 A and B show the electron density distributions using sign combinations, scaling factors, and origin reflections obtained from the results of the last two com-

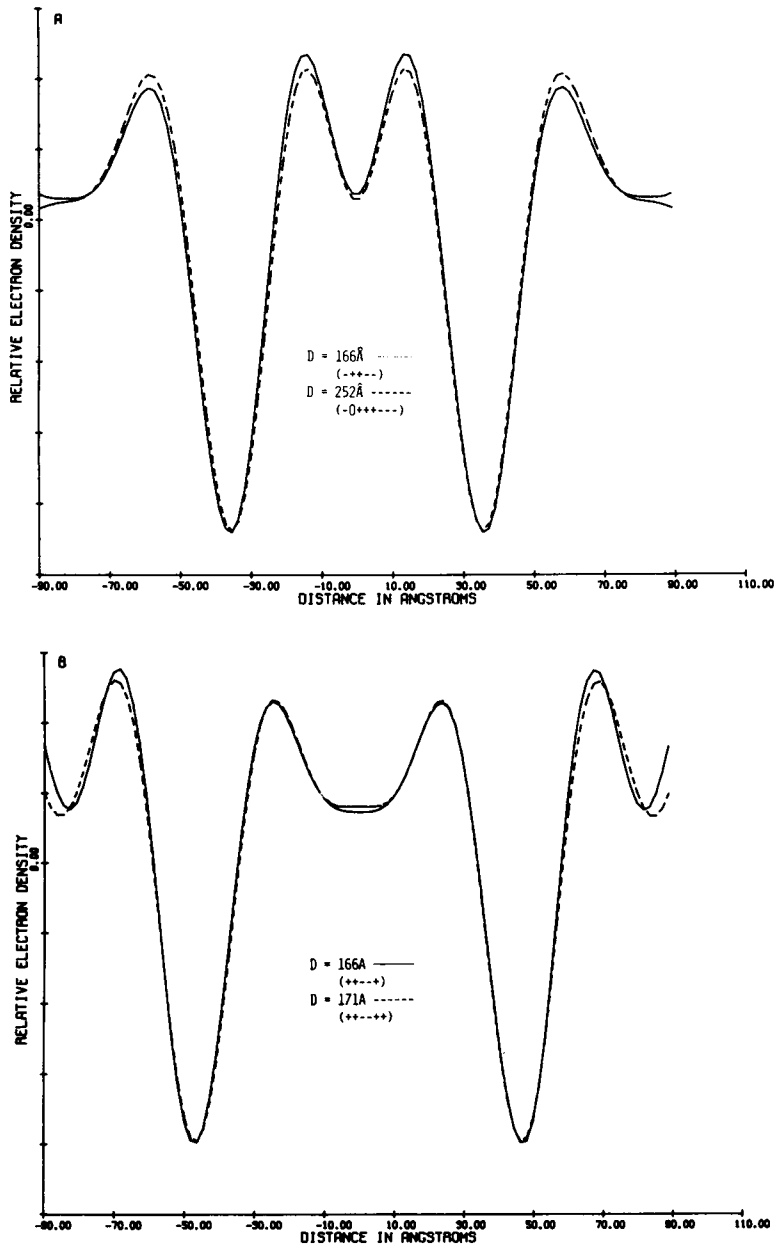


FIGURE 1 The projected electron density distribution of myelin at low resolution computed from intensity data by Blaurock (1967). The signs of the reflections, scaling factors, and origin reflection values are from the results shown in Table VII. Both are Calcomp plots. (A) Results of the second calculation in Table VII are used. The plot has an origin consistent with extracellular swelling. (B) Results of the third calculation in Table VII are used. The plot has an origin consistent with cytoplasmic swelling.

parisons shown in Table VII, and demonstrate the degree to which the condition of consistency of  $\rho(z)$  is satisfied by the correct sign choices. Numerical values of intensities for new and extensive myelin data (McIntosh and Worthington, 1974; Worthington and McIntosh, 1974) have not been published and should be used in this calculation.

### CONCLUSION

A method of phase determination has been developed for symmetric one-dimensionally periodic structures in which sign combinations, scaling factors, and origin reflection values can be calculated independently of one another from observed intensity data. This method is very rapid and has several advantages over previously reported methods, including, (a) the use of scaling factors which are subject only to experimental and truncation errors and are not approximated by the neglect of the origin reflection; (b) phase determination which is independent of consistency of calculated origin reflection values (which are subject to large variation due to experimental or truncation errors) and independent of approximated scaling factors; (c) rapid testing of all possible sign combinations; and (d) the use of the deviation,  $\Delta$ , as an analytical parameter to judge the consistency (and therefore, as a result of the assumption, the correctness) of particular sets of sign combinations (some of which may be insignificantly different from one another).

The method may be extended to large numbers of reflections by performing the calculation for the first several reflections and then continuing with higher orders while holding the original sign combinations fixed. The method has also been extended to cover situations in which the intermembrane fluid density changes from one sample to another (Stamatoff, 1974). In this case the plot is performed over the intramembrane region (to be published).

The authors thank Dr. Jean P. Krusch for the valuable contributions made during several discussions.

This research was supported in part by National Science Foundation grant BMS74-21163, and by a Macromolecular Research Center fellowship to J. B. Stamatoff.

Received for publication 10 March 1975 and in revised form 14 July 1975.

### REFERENCES

1. BLAUROCK, A. E. 1967. Ph.D. Thesis. University of Michigan, Ann Arbor.
2. BLAUROCK, A. E. 1971. Structure of the nerve myelin membrane: proof of the low resolution profile. *J. Mol. Biol.* **56**:35.
3. CORLESS, J. M. 1972. Lamellar structure of bleached and unbleached rod photoreceptor membranes. *Nature (Lond.)* **237**:229.
4. HOSEMANN, R., and S. N. BAGCHI. 1962. Direct analysis of diffraction by matter. North-Holland Publishing Company, Amsterdam.
5. KING, G. I. 1971. Ph.D. Thesis. University of Michigan, Ann Arbor.
6. LUZZATI, V., A. TARDIEU, and D. TAUPIN. 1972. A pattern-recognition approach to the phase problem: application to the x-ray diffraction study of biological membranes and model systems. *J. Mol. Biol.* **64**:269.

7. MCINTOSH, T. J., and C. R. WORTHINGTON. 1974. Direct determination of the lamellar structure of peripheral nerve myelin at low resolution (17 Å). *Biophys. J.* **14**:363.
8. MOODY, M. F. 1974. Structure determination of membranes in swollen lamellar systems. *Biophys. J.* **14**:697.
9. PAPE, E. H. 1974. X-ray small angle scattering, a new deconvolution method for evaluating electron density distributions from small angle scattering diagrams. *Biophys. J.* **14**:284.
10. RAND, R. P., and V. LUZZATI. 1968. X-ray diffraction study in water of lipids extracted from human erythrocytes, the position of cholesterol in the lipid lamellae. *Biophys. J.* **8**:125.
11. SCHWARTZ, S., J. E. CAIN, E. DRATZ, and J. K. BLASIE. 1974. An analysis of lamellar diffraction from disordered membrane multilayers with application to data from retinal rods. *Fed. Proc.* **33**:1575.
12. STAMATOFF, J. B. 1974. Ph.D. Thesis, University of Michigan, Ann Arbor.
13. STAMATOFF, J. B., S. KRIMM, and N. R. HARVIE. 1975. X-ray diffraction studies of human erythrocyte membrane structure. *Proc. Natl. Acad. Sci. (U.S.A.)*. **72**:531.
14. WORTHINGTON, C. R., and G. I. KING. 1971. Electron density profiles of nerve myelin. *Nature (Lond.)*. **234**:143.
15. WORTHINGTON, C. R., G. I. KING, and T. J. MCINTOSH. 1973. Direct structure determination of multi-layered membrane-type systems which contain fluid layers. *Biophys. J.* **13**:480.
16. WORTHINGTON, C. R., and T. J. MCINTOSH. 1974. Direct determination of the lamellar structure of peripheral nerve myelin at moderate resolution (7 Å). *Biophys. J.* **14**:703.